

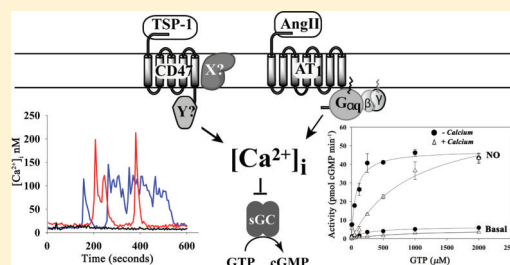
# Thrombospondin-1 and Angiotensin II Inhibit Soluble Guanylyl Cyclase through an Increase in Intracellular Calcium Concentration

Saumya Ramanathan,<sup>†</sup> Stacy Mazzalupo,<sup>‡</sup> Scott Boitano,<sup>§</sup> and William R. Montfort<sup>\*,‡</sup>

<sup>†</sup>Department of Molecular and Cellular Biology, <sup>‡</sup>Department of Chemistry and Biochemistry, and <sup>§</sup>Department of Physiology and The Arizona Respiratory Center, University of Arizona, Tucson, Arizona 85721, United States

**S** Supporting Information

**ABSTRACT:** Nitric oxide (NO) regulates cardiovascular hemostasis by binding to soluble guanylyl cyclase (sGC), leading to cGMP production, reduced cytosolic calcium concentration ( $[Ca^{2+}]_i$ ), and vasorelaxation. Thrombospondin-1 (TSP-1), a secreted matricellular protein, was recently discovered to inhibit NO signaling and sGC activity. Inhibition of sGC requires binding to cell-surface receptor CD47. Here, we show that a TSP-1 C-terminal fragment (E3CaG1) readily inhibits sGC in Jurkat T cells and that inhibition requires an increase in  $[Ca^{2+}]_i$ . Using flow cytometry, we show that E3CaG1 binds directly to CD47 on the surface of Jurkat T cells. Using digital imaging microscopy on live cells, we further show that E3CaG1 binding results in a substantial increase in  $[Ca^{2+}]_i$ , up to 300 nM. Addition of angiotensin II, a potent vasoconstrictor known to increase  $[Ca^{2+}]_i$ , also strongly inhibits sGC activity. sGC isolated from calcium-treated cells or from cell-free lysates supplemented with  $Ca^{2+}$  remains inhibited, while addition of kinase inhibitor staurosporine prevents inhibition, indicating inhibition is likely due to phosphorylation. Inhibition is through an increase in  $K_m$  for GTP, which rises to 834  $\mu$ M for the NO-stimulated protein, a 13-fold increase over the uninhibited protein. Compounds YC-1 and BAY 41-2272, allosteric stimulators of sGC that are of interest for treating hypertension, overcome E3CaG1-mediated inhibition of NO-ligated sGC. Taken together, these data suggest that sGC not only lowers  $[Ca^{2+}]_i$  in response to NO, inducing vasodilation, but also is inhibited by high  $[Ca^{2+}]_i$ , providing a fine balance between signals for vasodilation and vasoconstriction.



Nitric oxide (NO) regulates numerous vital functions in animal physiology including blood pressure, memory formation, platelet aggregation, angiogenesis, and tissue development.<sup>1</sup> Dysregulation of NO signaling contributes to cardiovascular disease, difficulties in wound healing, diabetes, asthma, and aging. NO is produced through the conversion of L-arginine to L-citrulline by nitric oxide synthase (NOS)<sup>2,3</sup> and may function in the same cell where it is produced and/or in nearby cells (autocrine/paracrine signaling). Three isoforms of NOS are found in mammals, endothelial NOS (eNOS), neuronal NOS (nNOS), and inducible NOS (iNOS). Both eNOS and nNOS are regulated by  $Ca^{2+}$  through its binding to calmodulin. The primary NO receptor is soluble guanylyl/guanylate cyclase (sGC), a heterodimeric protein of ~150 kDa that binds NO through a ferrous heme. NO binding stimulates cyclase activity, the production of cGMP from substrate GTP, and the subsequent amplification of NO-dependent signaling cascades.<sup>4–7</sup> In smooth muscle cells, this leads to a reduction in cytosolic calcium concentration ( $[Ca^{2+}]_i$ ) and smooth muscle relaxation, a mechanism closely tied to the regulation of blood pressure. While regulation of NOS is relatively well studied,<sup>8</sup> the mechanisms underlying sGC regulation are poorly understood.<sup>4</sup>

Recently, thrombospondin-1 (TSP-1), a trimeric extracellular matrix protein of 450 kDa, was discovered to be an inhibitor of NO signaling.<sup>9</sup> The NO-stimulated increase in endothelial cell proliferation, migration, and adhesion, which are of importance for angiogenesis, wound healing, and tumor progression, are

potently blocked by TSP-1. TSP-1 also blocks smooth muscle relaxation, leading to vasoconstriction. The mechanisms behind TSP-1 attenuation of NO signaling are not yet known but involve inhibition at multiple steps, including those involving vascular endothelial growth factor receptor-2 (VEGFR2), eNOS, sGC, and protein kinase G (PKG).<sup>10,11</sup> Among these, inhibition of sGC is particularly prominent and the focus of the present investigation.

TSP-1 is a multidomain protein consisting of a globular N-terminal domain, procollagen homology domain, three thrombospondin structural or properdin-like (type 1) repeats, three EGF-like (type 2) repeats, seven  $Ca^{2+}$ -binding (type 3) repeats, and a globular C-terminal cell-binding domain (Figure 1).<sup>12–14</sup> The trimeric form of the protein is stabilized through disulfide bonds located just after the N-terminal domain. TSP-1 interacts with multiple cell surface receptors through each of its domains and elicits a multitude of physiological responses. Through its C-terminal domain, TSP-1 binds to CD47 (also called integrin-associated protein; IAP), which is required for sGC inhibition.<sup>9</sup>

CD47 is an ~50 kDa integral-membrane protein expressed in most cell types. It is suspected to traverse the membrane five

**Received:** June 2, 2011

**Revised:** August 3, 2011

**Published:** August 8, 2011



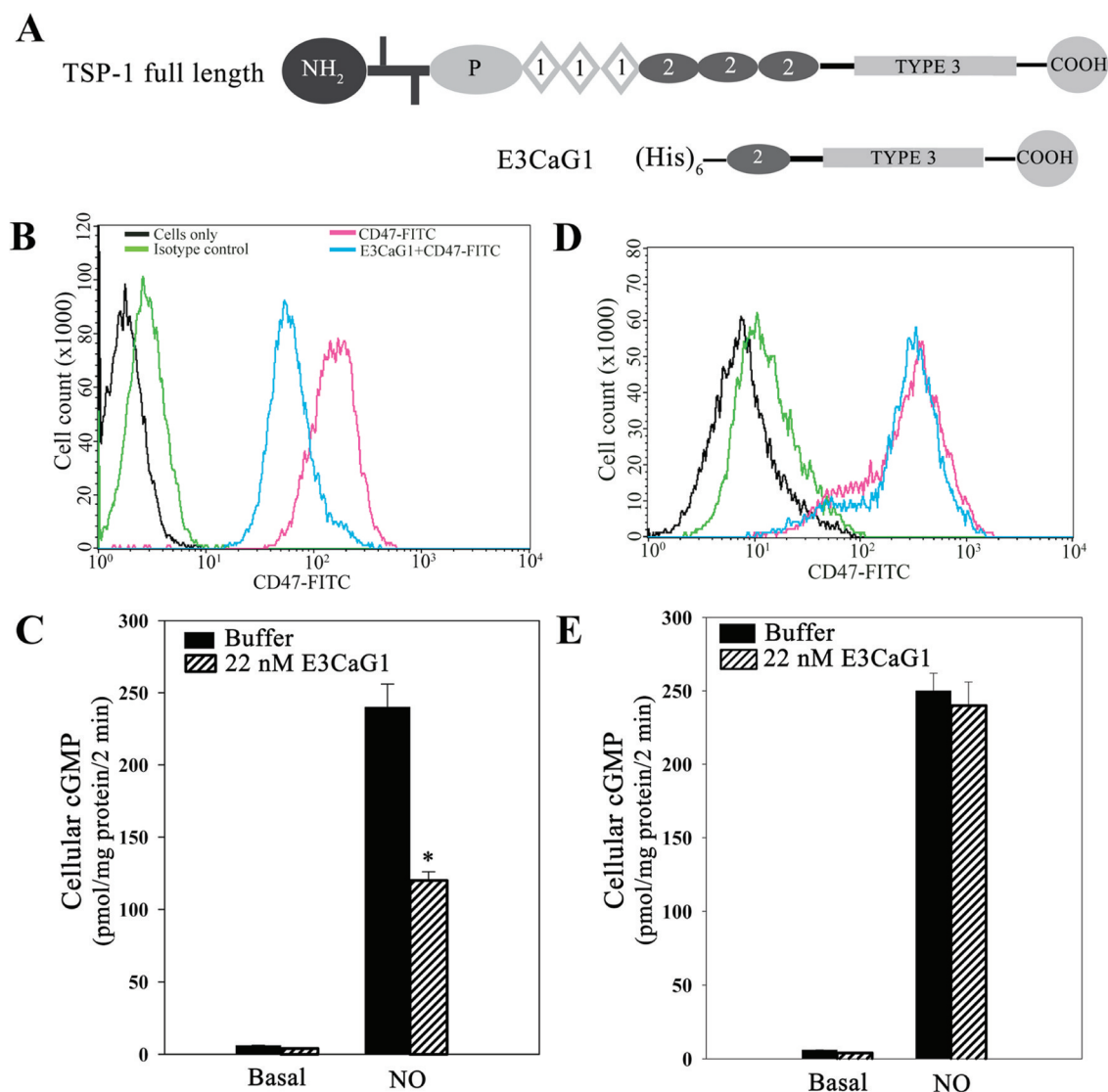


**Figure 1.** E3CaG1 binding to Jurkat T cells and inhibition of sGC. (A) Schematic diagrams of full-length TSP-1 and the recombinant C-terminal fragment used in this study (E3CaG1). N-terminal, C-terminal, procollagen, and type 1–3 domains are indicated. Two bars near the N-terminus indicate the cysteines involved in disulfide linkage. (B) Flow cytometry histogram of Jurkat T cells labeled with FITC-conjugated anti-human CD47 antibody in the presence or absence of E3CaG1, or with isotype or vehicle control, as indicated.  $1 \times 10^6$  cells were used per condition. Young cells (<2 weeks in culture) grown at low densities ( $0.5 \times 10^6$  cells/mL) were used; where indicated, cells were incubated with E3CaG1 prior to the addition of the anti-CD47 antibody. (C) Young Jurkat T cells were examined for cGMP production ( $1 \times 10^6$  cells per assay condition). Where indicated, cells were incubated with E3CaG1 at room temperature (15 min), followed by the addition of  $10 \mu\text{M}$  DEA/NO. Error bars represent the standard deviation from mean of independent experiments ( $n = 5$ ), and \* denotes  $p < 0.001$ . (D) and (E) are as in (B) and (C), except that older cells (>6 weeks in culture), grown to greater densities ( $3 \times 10^6$  cells/mL), were used. Only in the younger cells was E3CaG1 able to compete with binding by the CD47 antibody and inhibit NO-stimulated sGC activity.

times and has an IgV-like extracellular domain and a small alternatively spliced intracellular domain.<sup>15</sup> The two well-characterized ligands of CD47 are signal inhibitory receptor protein  $\alpha$  (SIRP $\alpha$ ) and TSP-1. The CD47/SIRP $\alpha$  interaction functions to regulate innate immunity and experiments using knockout mice reveal that CD47 could act as a “self” marker since lack of CD47 leads to cells being phagocytosed by macrophages.<sup>16</sup> CD47 can be coimmunoprecipitated with G-protein G<sub>i</sub><sup>17</sup> and is implicated in triggering G<sub>i</sub>-dependent apoptosis in both breast cancer cells<sup>18</sup> and T lymphocytes.<sup>19</sup> This has led to the suggestion that CD47 might be a noncanonical G-protein coupled receptor (GPCR) and that CD47/integrin complexes mimic GPCRs.<sup>15,20</sup> When TSP-1 binds to CD47 at the cell surface, there is a decrease in cGMP

production due to the reduced ability of NO to stimulate sGC. Full length TSP-1, a peptide derived from the C-terminus of TSP-1 (4N1), and a C-terminal fragment of TSP-1 (E3CaG1) have all been shown to inhibit NO signaling through a reduction in sGC activity.<sup>9,10</sup> Previous studies indicate that TSP-1 inhibition of NO signaling is directly through sGC and not, for example, through inhibition of phosphodiesterases.<sup>21,22</sup> Additionally, 4N1 or 4N1K (modified 4N1) and TSP-1 binding to CD47 have each been shown to increase  $[\text{Ca}^{2+}]_i$  levels in mast cells<sup>23</sup> and fibroblasts.<sup>24</sup>

sGC is a heterodimeric enzyme with one  $\alpha$  subunit of ~77 kDa and one heme-containing  $\beta$  subunit of ~70 kDa. Each subunit consists of an N-terminal H-NOX domain, central PAS and coiled-coil domains, and a C-terminal catalytic

domain.<sup>25</sup> Subcellular localization,<sup>26,27</sup> dimerization status,<sup>28</sup> phosphorylation,<sup>29–34</sup> protein–protein interaction,<sup>35–38</sup> S-nitrosation<sup>39,40</sup> and  $[Ca^{2+}]_i$  levels<sup>41–43</sup> have all been implicated in sGC regulation. Calcium, nitric oxide, and cGMP are intimately associated in controlling numerous cellular functions, especially vascular tone. High  $[Ca^{2+}]_i$  levels lead to attenuation of NO-induced cGMP accumulation in transformed HEK 293 cells,<sup>41</sup> in primary astrocytes,<sup>44</sup> and in primary pituitary gland cells,<sup>45</sup> and micromolar calcium concentrations can directly inhibit isolated sGC.<sup>41,42,46</sup>

On the basis of the foregoing, we hypothesized that TSP-1 inhibition of sGC was mediated through  $Ca^{2+}$  signaling. Here, we show that E3CaG1 binding to Jurkat T cells leads to an increase in  $[Ca^{2+}]_i$  and that this pulse is required for inhibition of sGC. We also show that a potent vasoconstrictor, angiotensin II (Ang II), which induces an increase in  $[Ca^{2+}]_i$  through GPCR AT<sub>1</sub>,<sup>47,48</sup> also inhibits sGC through a  $Ca^{2+}$ -dependent mechanism.

## MATERIALS AND METHODS

**Materials.** FITC-conjugated monoclonal antihuman CD47 antibody (B6H12) and an isotype control antibody were obtained from BD Biosciences (San Jose, CA). Anti-integrin antibodies to  $\alpha V$  (P2W7 and 272-17E6) were obtained from Abcam. Ionomycin, thapsigargin, PHA, and BAPTA-AM were obtained from Invitrogen (Carlsbad, CA). Fura-2AM was obtained from CalBiochem/EMD Biosciences (San Diego, CA). 2-(*N,N*-Diethylamino)diazenolate-2-oxide (DEA/NO) was a kind gift from Dr. Katrina Miranda (University of Arizona). Phosphate-buffered saline (PBS) was prepared as 10 mM  $KH_2PO_4$ , 10 mM  $Na_2HPO_4$ , 137 mM NaCl, 2.7 mM KCl, pH 7.4. Tris-buffered saline (TBS) was prepared as 10 mM Tris-HCl, 150 mM NaCl, pH 7.4. Krebs buffer was prepared as 25 mM HEPES, 120 mM NaCl, 4.75 mM KCl, 1.44 mM  $MgSO_4$ , 11 mM glucose, pH 7.4. All other reagents were obtained from Sigma unless otherwise noted.

**Cell Culture.** Sf9 cells were maintained in Grace's Insect Media (Invitrogen) supplemented with 10% fetal bovine serum (Atlanta Biologicals), gentamicin (10 mg/mL), and fungizone (0.25  $\mu g/mL$ ). Jurkat T cells (TIB-152) were purchased from ATCC. Jurkat T cells lacking CD47 (JinB8<sup>49</sup>) or integrin  $\beta 1$  (Jurkat A1<sup>50</sup>) were the kind gift of Dr. David Roberts (NIH). All Jurkat cell lines were maintained in RPMI 1640 (Invitrogen) supplemented with 5% fetal bovine serum (FBS), penicillin (5 mg/mL), and streptomycin (1 mg/mL). Jurkat T cells were maintained below  $2 \times 10^6$  cells/mL, unless otherwise noted, and were weaned from 5% FBS to serum-free conditions starting 48 h prior to all experiments. 3T3 L1 fibroblasts were the kind gift of Dr. Tsu-Shuen Tsao (University of Arizona) and were maintained in DMEM (Invitrogen) supplemented with 10% FBS, penicillin (5 mg/mL), and streptomycin (1 mg/mL). MCF-7 cells were obtained from ATCC (HTB-22) and maintained in DMEM supplemented with 10% FBS, penicillin (5 mg/mL), and streptomycin (1 mg/mL) and used for experiments within 10 passages after thawing.

**Flow Cytometry.**  $1 \times 10^6$  Jurkat T cells resuspended in stain/wash buffer (PBS supplemented with 0.1% BSA, 0.01%  $NaN_3$ ) were used per assay condition. Cells were incubated with stain/wash buffer or stain/wash buffer supplemented with E3CaG1 (22 nM) for 1 h at 4 °C and were fixed with 4% paraformaldehyde prior to incubation with FITC-conjugated

monoclonal antihuman CD47 antibody or isotype control. Cells were washed with stain/wash buffer to remove unbound antibody followed by addition of 4% paraformaldehyde. One-color flow cytometric analysis was performed at 488 nm using a FACScan flow cytometer (BD Biosciences). The emission fluorescence of FITC-conjugated CD47 antibody was detected using a 530/30 bandpass filter and recorded at a rate of 200–400 events/s for 10 000 events gated on FSC (forward scatter) vs SSC (side scatter). Data were analyzed using CellQuest PRO software (BD Biosciences). Appropriate electronic compensation was adjusted by acquiring cell populations stained with each dye/fluorophore individually, as well as an unstained control.

To examine increased  $[Ca^{2+}]_i$  by flow cytometry, we loaded cells with 5  $\mu M$  Fluo-3AM in Krebs buffer for 30 min at room temperature with gentle mixing every 10 min. The green fluorescence emission of calcium binding dye Fluo-3 was then analyzed following 488 nm laser excitation on a BD LSRII flow cytometer (Becton Dickinson, Inc.). Buffer or E3CaG1 (2.2–220 nM) was added to cell suspension ( $2 \times 10^6$  cells/500  $\mu L$ ), and data were collected after 10 min. Where indicated, cells were incubated with anti-CD47 antibody (B6H12) for 20 min prior to the addition of E3CaG1. Data were analyzed using FlowJo (v.7.6.4).

**Expression and Purification of E3CaG1.** Baculoviral vector pAcGP67.coco (COCO), encoding E3CaG1, was kindly provided by Dr. Deane Mosher (University of Wisconsin). Expression and purification were carried out as described.<sup>51</sup> Briefly, Sf9 cells were grown at 27 °C and were maintained in Grace's Insect Media supplemented with 10% fetal bovine serum and gentamicin and fungizone. When the cells reached a density of  $1 \times 10^6$  cells/mL, they were transferred to SF900II media (Invitrogen) and were infected with high titer virus at a multiplicity of infection of 5. Media was collected 65 h postinfection. After the His-tagged E3CaG1 was purified by immobilized metal ion affinity chromatography, it was stored at –80 °C in TBS supplemented with 2 mM  $CaCl_2$ . Protein concentrations were determined by the BCA assay (Thermo Scientific, Rockford, IL) using bovine serum albumin as the standard.

**Cloning and Transient Transfection of Human Soluble Guanylyl Cyclase.** Primers 5'-ctcagtctcgagatctattctgatgc-3' and 5'-cagtcaggatccgagtggtctgcacgaagc-3' were used to amplify human sGC  $\alpha 1$  cDNA (ATCC clone MGC-33150) for cloning into pCMV-3Tag-9 (Clontech, Mountain View, CA) between *Bam*HI and *Hind*III sites, yielding a C-terminal myc-tagged protein (vector WM397). Human sGC  $\beta 1$  was cloned into pCMV-3Tag-3A (Clontech) between *Sac*I and *Xho*I sites, yielding a C-terminal FLAG-tagged protein (vector WM434). Primers 5'-gcactcgaggtcatcatctgcttg-3' and 5'-cactgtgagctcatgtacggattgtg-3' were used to amplify the cDNA from plasmid pSTBlue1-Hu $\beta 1$  bearing the human sGC  $\beta 1$  cDNA—a gift from Dr. Alan Nighorn (University of Arizona). The Stratagene QuikChange Lightning Site-Directed Mutagenesis Kit (Agilent, La Jolla, CA) was used to correct all errors in both plasmids to match CCDS34085.1 (GUCY1A3) and CCDS47154.1 (GUCY1B3).<sup>52</sup> Transfection reagent TurboFect (Fermentas, Glen Burnie, MD) was used at a ratio of 20  $\mu g$  of plasmid DNA (1:1 ratio of sGC $\alpha$ :sGC $\beta$ ) to 25  $\mu L$  of reagent per 10 cm dish of cells at 50% confluency. Cells were harvested by trypsinization 12 h after transfection, and the cell pellet was quickly frozen in liquid nitrogen.

**sGC Immunoprecipitation and Activity Assays.** Transiently transfected MCF-7 cells were trypsinized and



resuspended in Krebs buffer. To manipulate  $[Ca^{2+}]_i$ , cells were incubated with ionomycin (1  $\mu$ g/mL), thapsigargin (400 nM), and 0.1 mM  $CaCl_2$  or vehicle control (DMSO) for 15 min. Cell pellets were lysed into homogenization buffer (50 mM Tris-HCl pH 7.5, 100 mM NaCl, 1 mM EDTA, 1 mM TCEP, 1 mM PMSF, protease inhibitor cocktail (10  $\mu$ L/mL cell lysate)) using a homogenizer. Lysate was spun at 13000g, and supernatant was combined with anti-FLAG agarose beads (Sigma, St. Louis, MO) for 1 h, 4 °C, on an Adams Nutator Mixer (BD Biosciences). After incubation, beads were washed with TBS and evenly divided into 0.6 mL Eppendorf tubes for the sGC activity assays. Inclusion of equal quantities of immunoprecipitated sGC in each assay condition was confirmed by Western blot analysis (Supporting Information Figure S1). Western blots were analyzed on an Odyssey Imaging System (LI-COR), and Image J software was used to analyze loading quantities. Reactions were carried out in a final volume of 100  $\mu$ L containing reaction buffer (3 mM GTP, 8 mM  $MgCl_2$ , 50 mM Hepes, pH 7.7, prepared at 10 $\times$  concentration just prior to use) and, where indicated, 10  $\mu$ M YC-1 or BAY 41-2272 or vehicle control, and 10  $\mu$ M DEA/NO. YC-1 and BAY 41-2272 were dissolved in DMSO and then diluted to a final stock concentration of 1.1 mM in ethanol. DEA/NO was prepared as a 1 mM stock solution in 10 mM NaOH. Upon adding DEA/NO or vehicle control, the assay was allowed to proceed for 5 min at 37 °C. The reactions were stopped by pelleting the beads and transferring the supernatant to Cell Lysis Buffer (Molecular Devices, Sunnyvale, CA, or Cisbio, Bedford, MA). cGMP concentrations were determined by competitive ELISA using the CatchPoint cGMP assay (Molecular Devices), following the manufacturer's instructions, or the homogeneous time-resolved fluorescence (HTRF) assay (Cisbio), following the manufacturer's instructions and using a BioTek H1F plate reader.

For kinetic measurements, transiently transfected MCF-7 cells were either treated with DMSO (vehicle control) or ionomycin, thapsigargin, and 2 mM  $CaCl_2$  for 5 min. Cell pellets were lysed as described above and incubated with anti-FLAG agarose beads for 1.5 h at 4 °C. Following this, the beads were washed three times and resuspended in an appropriate volume of Tris-buffered saline (pH 7.5). Aliquots of this slurry were then used for activity measurements. Reactions were carried out at 37 °C in a final volume of 150  $\mu$ L and initiated by the addition of reaction buffer (5–2000  $\mu$ M GTP, 8 mM  $MgCl_2$ , 50 mM HEPES, pH 7.5, prepared at 10 $\times$  concentration just prior to use). Where NO-induced sGC activities were measured, DEA/NO (50  $\mu$ M) was added immediately after the addition of reaction buffer. Reactions were quenched by the addition of cell lysis buffer from the cGMP kit, generally after 10 min (–NO) or 3 min (+NO). Catalytic rates were linear over these time periods for all GTP concentrations used. Inclusion of equal quantities of immunoprecipitated sGC was confirmed by Western blot analysis (Supporting Information Figure S1). For each experiment, cGMP accumulation was measured in duplicate using the cGMP-ELISA kit from Molecular Devices or the HTRF kit from Cisbio; higher concentrations of GTP did not interfere with the measurements. Kinetic parameters were obtained by nonlinear fitting of the Michaelis–Menten equation, using SigmaPlot (SPSS, Inc., Chicago, IL).  $K_m$  and  $V_{max}$  are presented as the average and standard deviation of three independent experiments.

**sGC Activity and cGMP Accumulation in Intact Cells and Cell Lysates.** Jurkat T cells ( $1 \times 10^6$  per assay condition)

were resuspended in Krebs buffer. Where indicated, cells were preincubated with treatment agents (E3CaG1, BAPTA-AM, etc.) or vehicle controls for the indicated time at room temperature, followed by addition of 10  $\mu$ M DEA/NO. Reactions were stopped after 2 min by placing the cell suspensions on ice, pelleted, and quickly frozen. For cGMP measurements, the cell pellets were thawed and resuspended with 100  $\mu$ L of Cell Lysis Buffer. The basal and NO-induced sGC activities of intact cells were expressed in terms of picomoles of cGMP produced per minute per milligram of total protein content (pmol cGMP  $min^{-1} mg^{-1}$ ), using the CatchPoint cGMP assay kit. Protein concentrations were determined by the BCA assay (Thermo Scientific) using bovine serum albumin as the standard.

To examine E3CaG1 inhibition, cells were incubated with 22 nM E3CaG1 in Krebs buffer for 15 min at room temperature, followed by the addition of 10  $\mu$ M DEA/NO. To manipulate  $[Ca^{2+}]_i$ , cells were incubated with ionomycin (1  $\mu$ g/mL) and thapsigargin (400 nM), 20 mM EGTA or vehicle control, and 0–10 mM  $CaCl_2$  for 15 min, followed immediately by addition of 10  $\mu$ M DEA/NO. For experiments examining intracellular calcium chelation, cells were incubated with BAPTA-AM (10  $\mu$ M, added from a 2 mM stock solution in DMSO) or vehicle control for 15 min prior to the addition of E3CaG1 (16 nM) or buffer for 15 min, and then DEA/NO (10  $\mu$ M for 2 min). BAPTA-AM is a membrane permeable  $Ca^{2+}$  chelator that is converted to BAPTA in the cytosol, where it becomes trapped.

To examine the effect of PHA or Ang II on sGC activity, Jurkat T cells were grown in serum-free media 12 h prior to the experiment at a density of less than  $1 \times 10^6$  cells/mL. Where indicated, cells were incubated with 5  $\mu$ M BAPTA-AM or vehicle control (DMSO) for 15 min, followed by the addition of the indicated concentrations of PHA or 1  $\mu$ M Ang II for an additional 2 min, and then DEA/NO (10  $\mu$ M) for 2 min. To examine the effect of compounds YC-1 and BAY 41-2272 on E3CaG1 inhibition of sGC, cells were incubated with 22 nM E3CaG1 for 15 min prior to the addition of 10  $\mu$ M YC-1, 10  $\mu$ M BAY41-2272, or vehicle control, followed immediately by addition of DEA/NO.

To examine the effect of phosphodiesterases on cGMP accumulation in intact cells, MCF-7 cells transiently transfected with sGC were used. 14 h post-transfection, cells were trypsinized and incubated with vehicle/DMSO, IBMX (0.5 mM), or 8-methoxymethyl IBMX (0.4 mM) for 30 min, followed by addition of ionomycin (1  $\mu$ g/mL), thapsigargin (400 nM), and calcium chloride (0.1 mM) to appropriate samples, followed immediately by the addition of DEA/NO (10  $\mu$ M). After 2 min, cells were spun down and cell pellets frozen.

**Cell-Free Inhibition of sGC.** MCF-7 cells were transiently transfected with sGC; 14 h post-transfection, cells were trypsinized and pellets were lysed in homogenization buffer. Immunoprecipitation of sGC was performed as described above. Jurkat cell lysate was then incubated with the beads for 15 min at 37 °C with or without 250 nM  $Ca^{2+}$  and/or staurosporine (1  $\mu$ M). Following this, the beads were washed five times with TBS and resuspended in an appropriate volume for activity assay. Where indicated, 10  $\mu$ M DEA/NO and 10  $\mu$ M YC-1 were included in the reactions.

**sGC Activity and cGMP Accumulation in Lysed Jurkat T Cells.**  $25 \times 10^6$  Jurkat T cells were used for each assay condition and were incubated with buffer or E3CaG1. Cell pellets were lysed into 600  $\mu$ L of homogenization buffer (50 mM

Tris-HCl pH 7.5, 100 mM NaCl, 1 mM EDTA, 1 mM TCEP, 1 mM PMSF, protease inhibitor cocktail (10  $\mu$ L/mL cell lysate)) using a homogenizer. Lysate was spun at 13000g, and supernatant was incubated with or without IBMX (0.5 mM) and 8-methoxymethyl IBMX (0.4 mM) for 10 min. This was followed by the addition of Mg-GTP reaction buffer and DEA/NO (10  $\mu$ M). Reactions were stopped after 2 min by the addition of 250  $\mu$ L of cell lysis buffer (Molecular Devices, Sunnyvale, CA). cGMP concentrations were determined by competitive ELISA using the CatchPoint cGMP assay (Molecular Devices), following the manufacturer's instructions.

**Calcium Imaging.** In order to assay  $[Ca^{2+}]_i$  in Jurkat T cells, which normally grow in suspension, 3T3 L1 fibroblasts were used to coat glass coverslips with extracellular matrix. Fibroblasts were hypotonically lysed, and cellular debris was mechanically removed with a cell scraper. Jurkat T cells were then allowed to adhere to the matrix-coated coverslips. The cells were left undisturbed for a minimum of 1 h before use and remained attached to the coverslips under these conditions for up to 4 h. Attached cells were loaded with Fura-2AM for 30 min at room temperature in the dark. Fura-2 fluorescence was observed on an Olympus (Center Valley, PA) IX70 microscope equipped with a 75 W xenon lamp while alternating between excitation wavelengths of 340 and 380 nm. Images of emitted fluorescence above 505 nm were captured by an ICCD camera (Photon Technology International, Birmingham, NJ) under ImageMaster software control (PTI). Effective  $[Ca^{2+}]_i$  was calculated from equations published in ref 53. Initial  $[Ca^{2+}]_i$  was assessed over 20–60 s to establish a consistent baseline, and changes in  $[Ca^{2+}]_i$  were monitored over time for each experimental condition. Depending on the experiment, measurements were taken every 0.6 s (for 3–5 min experiments) up to 5 s (for experiments >5 min). Cell morphology within the time period of measurement was assessed by differential interference contrast microscopy and found not to vary.

**Statistical Analysis.** Data are presented as mean  $\pm$  SD of independent experiments. Differences between groups were compared for significance using Student's *t* test (calculated with Microsoft Excel software).

## RESULTS

**CD47 Is Necessary but Insufficient for E3CaG1 Binding to Jurkat T Cells and Inhibition of sGC.** To examine the mechanism behind TSP-1 inhibition of sGC, we used E3CaG1, a C-terminal TSP-1 construct that retains robust activity and is more stable than full-length TSP-1. E3CaG1 consists of the last EGF $\beta$ -like type II repeat, all of the calcium binding type III repeats, and the C-terminal cell-binding domain required for CD47-dependent activity (Figure 1A). We chose Jurkat T cells for these experiments since these cells are one of the few immortalized cell lines with intact sGC signaling and since they also respond to TSP-1.<sup>54</sup> Initial experiments with full-length TSP-1 suggested inconsistent inhibition of sGC activity (data not shown). To uncover the reason for this, we used E3CaG1 to study CD47 binding over time. We measured binding of E3CaG1 to Jurkat T cells through its ability to compete with a FITC-conjugated monoclonal antihuman CD47 antibody, using fluorescence activated cell sorting (FACS). We first examined cells that had been kept at low density ( $0.5 \times 10^6$  cells/mL) or that had been cultured for less than 2 weeks. These cells exhibited very little autofluorescence

and only a small increase in fluorescence upon treatment with a FITC-conjugated isotype control antibody, indicating little nonspecific binding occurs. When cells were incubated with the FITC-conjugated CD47 antibody, there was an  $\sim$ 100-fold increase in fluorescence, indicating the presence of CD47 on the surface of Jurkat T cells. Plots of scattering vs fluorescence for these data ("dot plots", Supporting Information Figure S2) indicated a homogeneous population of positively stained cells, consistent with a uniform distribution of CD47 throughout the Jurkat T cell population. When E3CaG1 (22 nM) was added to cells prior to the addition of CD47 antibody, the mean fluorescence decreased significantly, indicating that E3CaG1 competes with the monoclonal antibody and binds to CD47 on the Jurkat T cell surface (Figure 1B). Older cells (>6 weeks), or cells that had been grown at higher density ( $3 \times 10^6$  cells/mL), could still bind antibody, but E3CaG1 was no longer able to compete with antibody binding (Figure 1D).

Preparations of E3CaG1 had little effect on the basal activity of sGC in younger cells but profoundly inhibited NO-stimulated sGC activity (Figure 1C), much as previously reported in other cell types.<sup>9</sup> We observed strong inhibition for E3CaG1 concentrations as low as 0.22 nM (42%, Supporting Information Figure S3) and found inhibition to be maximal for concentrations above  $\sim$ 20 nM E3CaG1 ( $\sim$ 67%), similarly to previous reports for E3CaG1 and full-length TSP-1.<sup>9</sup> Subsequent experiments were performed with 22 nM E3CaG1.

When we examined older Jurkat T cells, no inhibition was seen (Figure 1E), consistent with the lack of binding as shown in Figure 1D. We conclude from these experiments that CD47 remains on the cell surface; however, CD47 or a complex that includes CD47 has changed and can no longer interact with the TSP-1 fragment. All subsequent experiments were therefore performed on cells that were within 3 weeks of growth and kept below  $1 \times 10^6$  cells/mL.

**E3CaG1 Induces an Increase in  $[Ca^{2+}]_i$ .** TSP-1 and peptide 4N1K are known to increase  $[Ca^{2+}]_i$  in fibroblasts and mast cells through a mechanism thought to require direct binding to CD47.<sup>23,24</sup> We hypothesized that E3CaG1 inhibition of sGC in Jurkat T cells also involved changes in  $[Ca^{2+}]_i$  and used digital imaging microscopy to examine this possibility (Figure 2, Supporting Information movie M1). Jurkat T cells were transferred to matrix-coated coverslips (see Materials and Methods) for these experiments and allowed to attach for at least 1 h, well beyond the time where attachment-associated  $Ca^{2+}$  spikes have previously been described, which persist for  $\sim$ 8 min postattachment.<sup>55</sup> At rest, Jurkat T cells displayed an  $[Ca^{2+}]_i$  of 10–25 nM. Addition of E3CaG1 (22 nM final concentration) induced an increase in  $[Ca^{2+}]_i$  to 150–300 nM (Figure 2A,B). Similar increases were not observed after washing with Hank's basal salt solution (HBSS, pH 7.4) alone (Figure 2B). Calcium concentrations could be experimentally controlled within Jurkat cells using the  $Ca^{2+}$  chelator BAPTA (Figure 2C) or the  $Ca^{2+}$  ionophore ionomycin and sarco/endoplasmic reticulum  $Ca^{2+}$  ATPase (SERCA) pump inhibitor thapsigargin (Figure 2D). None of the treatment conditions altered cell morphology within the time period of measurement as assessed by differential interference contrast microscopy.

**E3CaG1-Dependent Increases in  $[Ca^{2+}]_i$  Requires CD47.** We examined the requirement for CD47 using flow cytometry and the fluorescent  $Ca^{2+}$  indicator Fluo-3. Binding of 2.2 or 22 nM E3CaG1 to Jurkat T cells in suspension led to an  $\sim$ 100-fold increase in average fluorescence over addition of



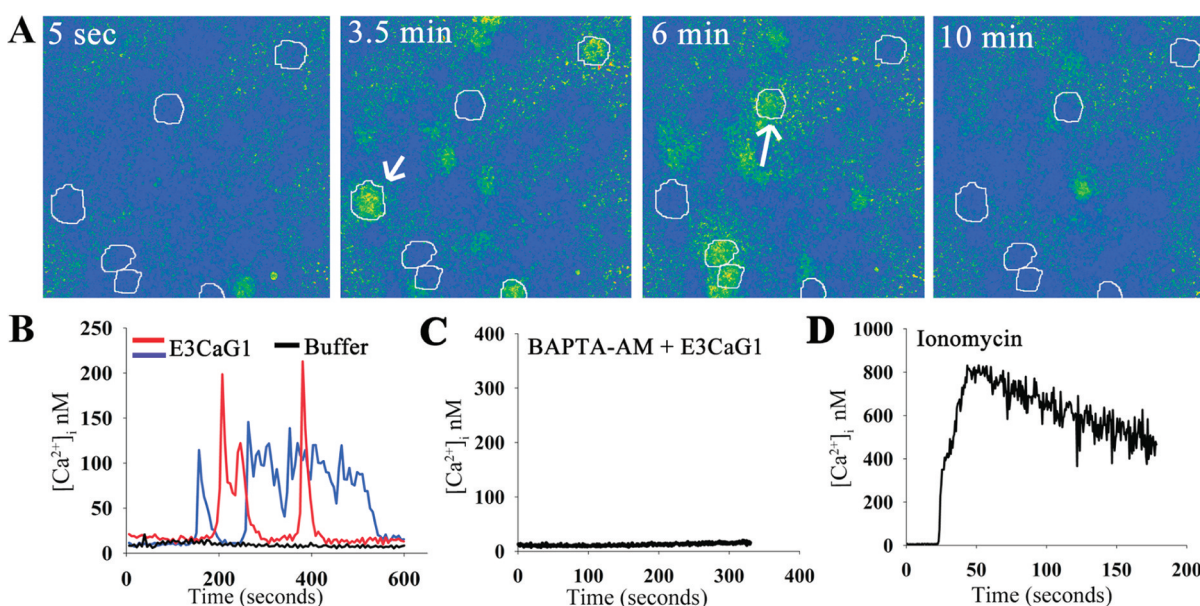


**Figure 2.** E3CaG1 induces increase of  $[Ca^{2+}]_i$  in Jurkat T cells. Jurkat T cells were attached to coverslips through an extracellular matrix laid down by fibroblasts, and  $[Ca^{2+}]_i$  was monitored over time using the calcium indicator Fura-2. (A) Snapshot of cells in the imaging field at individual time points over a 10 min experiment. The coloration indicates  $[Ca^{2+}]_i$  after addition of E3CaG1 (22 nM). Six Jurkat T cells of the 40 in the field of view are circled for emphasis. E3CaG1 induced peak  $[Ca^{2+}]_i$  in this and similar experiments range from 75 up to 300 nM. (B)  $[Ca^{2+}]_i$  traces over time for two representative cells (indicated with arrows in (A)). The black trace represents a typical cell response following addition of the vehicle control (HBSS buffer; from another experiment). (C)  $[Ca^{2+}]_i$  over time of a typical Jurkat T Cell following addition of E3CaG1 (22 nM) after preincubation (30 min) with BAPTA-AM (5  $\mu$ M) to effectively buffer  $[Ca^{2+}]_i$ . (D)  $[Ca^{2+}]_i$  over time of a typical Jurkat T Cell following addition of 2 mM extracellular  $CaCl_2$  in the presence of ionomycin (1  $\mu$ g/mL) and thapsigargin (400 nM).  $[Ca^{2+}]_i$  rises to 800 nM under these conditions.

buffer alone (Figure 3A). Thus, Jurkat T cells in suspension behaved similarly to those attached to coverslips. Addition of anti-CD47 antibody B6H12 completely blocked E3CaG1-dependent calcium mobilization. Likewise, cell line JinB8, which is a modified Jurkat T cell lacking CD47,<sup>49</sup> is not sensitive to E3CaG1 (Figure 3B). Similarly, antibody B6H12 abolishes E3CaG1-dependent inhibition of sGC (Figure 3C). We conclude that E3CaG1 signaling requires CD47, as expected from previous studies.<sup>9</sup> In contrast, antibodies to integrin  $\alpha V$ , which is known to associate with CD47,<sup>15</sup> have no effect on E3CaG1-dependent increases in  $[Ca^{2+}]_i$  (Supporting Information Figure S4) and subsequent inhibition of sGC (Figure 3C). E3CaG1 also remains active toward cell line Jurkat A1, which are integrin  $\beta 1$  null (data not shown).<sup>50</sup> Additionally, pertussis toxin, which inhibits Gi protein, had no effect on E3CaG1-dependent increases in  $[Ca^{2+}]_i$  (Supporting Information Figure S4) or on E3CaG1-dependent inhibition of cGMP production (data not shown).

**Calcium Inhibits NO-Inducible sGC Activity in Jurkat T Cells.** On the basis of previous reports showing that calcium can inhibit sGC activity in HEK 293 cells and also with purified protein,<sup>41,42,46</sup> we examined whether this was also the case for Jurkat T cells. Jurkat cells were resuspended in Krebs buffer containing 1  $\mu$ g/mL ionomycin and 400 nM thapsigargin and varying concentrations of extracellular calcium ( $[Ca^{2+}]_e$ ). Under these conditions,  $[Ca^{2+}]_i$  is effectively set by  $[Ca^{2+}]_e$ . NO-inducible cGMP accumulation was inversely proportional to  $[Ca^{2+}]_e$ , and complete inhibition occurred at  $[Ca^{2+}]_e = 4$  mM (Figure 4A). Chelating of extracellular calcium with EGTA abolished inhibition. Approximately 99% of cells were viable under each experimental condition, as indicated by trypan blue dye exclusion.

Chelating intracellular  $Ca^{2+}$  with compound BAPTA also overcame inhibition of sGC by E3CaG1, indicating that E3CaG1 inhibits sGC through a mechanism requiring increased  $[Ca^{2+}]_i$ . In the absence of BAPTA, E3CaG1 reduced NO-stimulated cGMP production by 50% (Figure 4B). However, after preloading the cells with BAPTA, E3CaG1 had no effect on cGMP production.

**Angiotensin II and Phytohemagglutinin Inhibit NO-Driven cGMP Accumulation.** Angiotensin II (Ang II) is a hormone that induces vasoconstriction through binding to GPCR  $AT_1$  and inducing a sustained increase in  $[Ca^{2+}]_i$  in targeted cells.<sup>47,48</sup> Phytohemagglutinin (PHA) is a natural agonist of the T-cell receptor that transiently increases  $[Ca^{2+}]_i$ .<sup>56</sup> Since Jurkat T cells have Ang II and T-cell receptors,<sup>56,57</sup> we asked whether Ang II and PHA would inhibit cGMP production by sGC. Addition of PHA inhibited NO-stimulated sGC activity in a dose-dependent manner to 60% at the highest concentration examined (50  $\mu$ g/mL, Figure 5A). Addition of 1  $\mu$ M Ang II to cells increased  $[Ca^{2+}]_i$  to a similar level as did E3CaG1 (Supporting Information Figure S4) and inhibited NO-stimulated sGC activity by 40% (Figure 5B). As with E3CaG1, chelating intracellular  $Ca^{2+}$  with BAPTA reversed this inhibition.

**Phosphodiesterases Have Minimal Effect.** Previous studies have indicated that TSP1-dependent inhibition of cGMP was through inhibition of sGC and not through stimulation of phosphodiesterases (PDEs).<sup>21,22</sup> To confirm that this was also true under the conditions of our experiments, we examined cGMP accumulation when PDE was inhibited. We first sought to directly inhibit PDE proteins in live Jurkat T cells using 3-isobutyl-1-methylxanthine (IBMX), a general PDE inhibitor, or 8-methoxymethyl IBMX, a specific inhibitor of calcium/calmodulin-dependent PDE1. Unfortunately, these

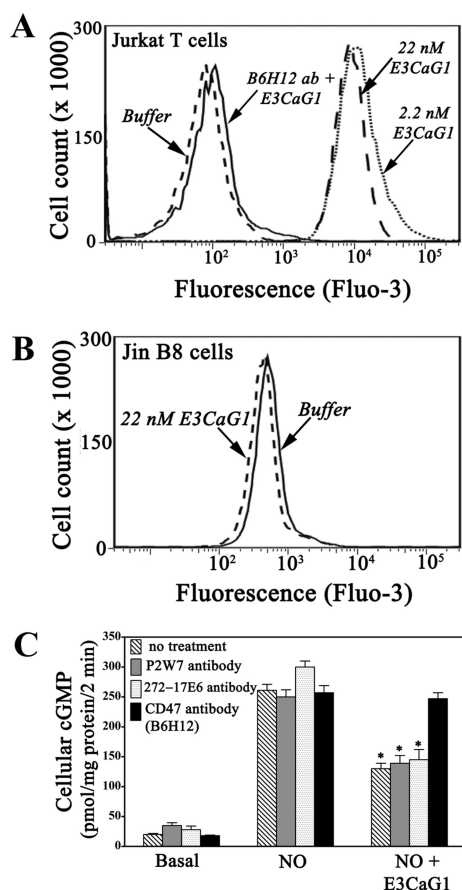


**Figure 3.** E3CaG1-induced increases in  $[Ca^{2+}]_i$  are cell adhesion independent but require CD47. (A) Flow cytometry histograms of green fluorescence emission by calcium binding dye Fluo-3. Addition of E3CaG1 (2.2 or 22 nM) to Jurkat T cells results in a 90–100-fold increase in Fluo-3 fluorescence over addition of buffer. Prior incubation with anti-CD47 antibody B6H12 eliminates E3CaG1-dependent increases in  $[Ca^{2+}]_i$ . (B) JinB8 cells that lack CD47 do not exhibit increases in intracellular calcium upon addition of E3CaG1. (C) Addition of anti-CD47 antibody B6H12 prevents E3CaG1-induced inhibition of sGC, whereas addition of anti-integrin  $\alpha V$  antibodies P2W7 or 272-17E6 prior to the addition of E3CaG1 does not. Jurkat T cells were incubated with respective antibodies for 30 min at 4 °C prior to the addition of E3CaG1 (22 nM). After 15 min, 10 mM NaOH (buffer control) or DEA/NO (10  $\mu$ M) was added as appropriate, followed by incubation for 2 min. Error bars represent the standard deviation from mean of independent experiments ( $n = 5$ ), and \* denotes  $p < 0.001$ .

compounds activate T cells, possibly through a cAMP-dependent mechanism,<sup>58</sup> which interferes with the measurement of E3CaG1 activity. We therefore measured NO-dependent cGMP accumulation in Jurkat T cell lysate obtained from cells that were previously treated with E3CaG1 or buffer control; measurements were made in the presence of IBMX or 8-methoxymethyl IBMX (Figure 6A). Under these conditions, calcium is diluted and PDEs inhibited. Inhibition of NO-stimulated sGC activity was pronounced in the cell-free lysate, consistent with only minor PDE effect on cGMP accumulation.

We further examined the role of PDEs using transiently expressed human sGC in MCF-7 cells, which do not normally express sGC. Raising  $[Ca^{2+}]_i$  in these cells led to pronounced inhibition of NO-stimulated sGC activity (Figure 6B). Addition of IBMX or 8-methoxy IBMX led to small increases in basal,

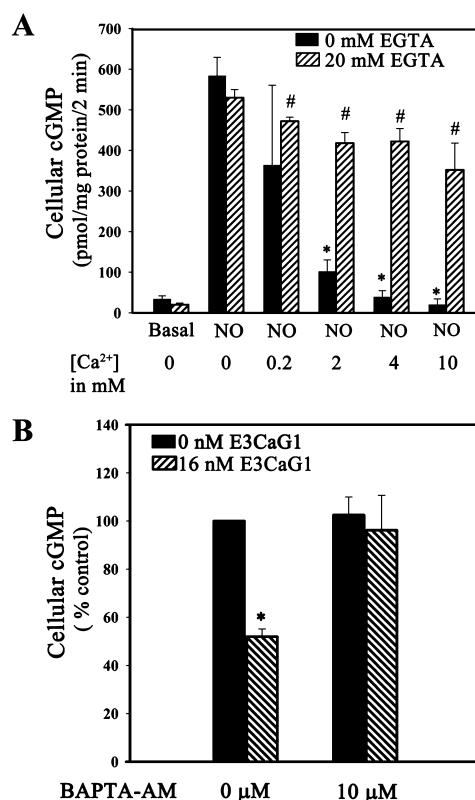


**Figure 4.** Increased  $[Ca^{2+}]_i$  leads to sGC inhibition in Jurkat T cells. (A) Manipulation of  $[Ca^{2+}]_i$  with ionomycin inhibits sGC. Jurkat T cells ( $1 \times 10^6$ ) were incubated with the  $Ca^{2+}$  ionophore ionomycin (1  $\mu$ g/mL) and the SERCA-inhibitor thapsigargin (400 nM) for 15 min at room temperature, followed by addition of EGTA (20 mM) or vehicle control, 0–10 mM  $CaCl_2$  as indicated, and 10  $\mu$ M DEA/NO. The reaction was stopped after 5 min. Error bars represent the standard deviation from the mean of independent experiments ( $n = 5$ ). \* denotes  $p < 0.001$ , and # denotes  $p < 0.5$ . (B) Chelating free cytosolic  $Ca^{2+}$  with cell permeable chelator BAPTA-AM reverses sGC inhibition by E3CaG1. Jurkat T cells ( $0.5 \times 10^6$ ) were incubated with 10  $\mu$ M BAPTA-AM or vehicle control (DMSO) 15 min prior to the addition of E3CaG1 (16 nM) or buffer and an additional 15 min incubation. This was followed by addition of DEA/NO (10  $\mu$ M); the reaction was stopped after 2 min cGMP accumulation was measured and expressed in terms of percentage control (10  $\mu$ M DEA/NO). Error bars represent the standard deviation from the mean of independent experiments ( $n = 4$ ), and \* denotes  $p < 0.001$ .

NO-stimulated, and calcium-inhibited cGMP levels; however, the 60% reduction in NO-stimulated cGMP accumulation due to increased  $[Ca^{2+}]_i$  was unchanged in the presence of these compounds, indicating PDEs have at most a minor role in the observed loss of cGMP under the conditions of our experiments.

**Compounds YC-1 and BAY 41-2272 Overcome  $Ca^{2+}$  Inhibition of sGC in Live Cells.** Compounds YC-1 and BAY 41-2272 are small molecule activators of sGC that act synergistically with NO and CO;<sup>59</sup> the related compound BAY 63-2521 (Riociguat) is in clinical trial for pulmonary hypertension.<sup>60</sup> When included at 10  $\mu$ M, E3CaG1 inhibition of NO-stimulated sGC was completely overcome by either YC-1 or BAY 41-2272 (Figure 7A,B), suggesting that  $Ca^{2+}$  inhibition of sGC is through an allosteric mechanism that can be overcome by allosteric stimulators. YC-1 also inhibits phosphodiesterases,<sup>61,62</sup> which may slightly contribute to the

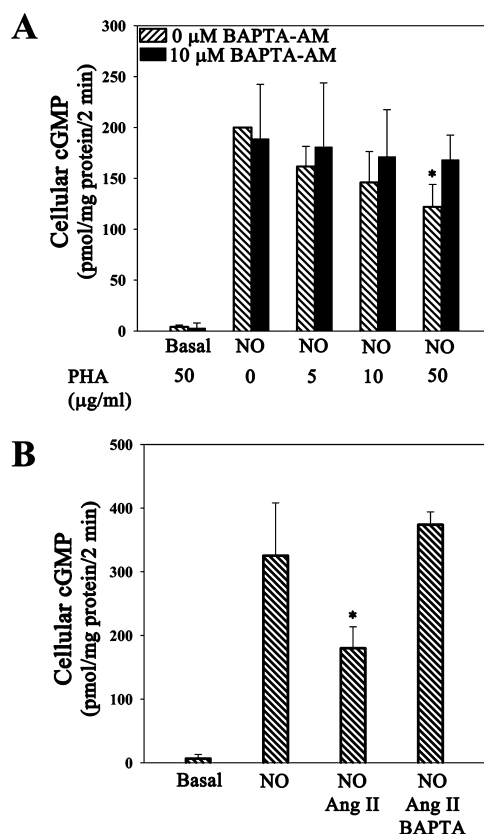


**Figure 5.** Stimulation of  $\text{Ca}^{2+}$  release by Ang II and PHA results in sGC inhibition. Jurkat T cells ( $0.5 \times 10^6$ ) were incubated with 5  $\mu\text{M}$  BAPTA-AM or vehicle control (DMSO) 15 min prior to the addition of indicated concentrations of PHA, Ang II (1  $\mu\text{M}$ ), or buffer and an additional 2 min incubation, followed by addition of DEA/NO (10  $\mu\text{M}$ ). The reaction was stopped after 2 min. Both PHA and Ang II inhibited sGC in the absence of BAPTA, but not in its presence. (A) PHA and (B) Ang II. Error bars represent the standard deviation from the mean of independent experiments ( $n = 5$ ), and \* denotes  $p < 0.01$ .

cGMP accumulation shown in Figure 7A. Although BAY 41-2272 can also inhibit phosphodiesterases,<sup>63</sup> inhibition is less pronounced<sup>64,65</sup> and unlikely to be a factor in Figure 7B.

**Immunoprecipitated sGC Remains Inhibited, but Activity Is Recovered upon Binding Compounds YC-1 and BAY 41-2272.** That sGC in diluted cell extracts remains inhibited (Figure 6A) suggests inhibition may be through covalent modification. To further examine this possibility, we transiently expressed human sGC in MCF-7 cells and isolated the protein through immunoprecipitation using a FLAG purification tag. The immunoprecipitated protein displays strong NO-stimulated activity (Figure 7C). However, when cells were first treated with  $\text{Ca}^{2+}$ /ionomycin, the isolated protein was substantially inhibited. As with cellular sGC, addition of YC-1 or BAY 41-2272 reversed the inhibition. Thus, higher  $[\text{Ca}^{2+}]_i$  leads to a modified sGC with reduced activity, and this activity can be overcome by allosteric stimulators.

Two reports indicate that  $\text{Ca}^{2+}$  can directly inhibit sGC isolated from bovine lung, with  $K_i$  values varying between 0.15 and 98.5  $\mu\text{M}$  depending on conditions and laboratory.<sup>42,46</sup> We examined direct inhibition of immunoprecipitated human sGC and found that addition of 100  $\mu\text{M}$   $\text{Ca}^{2+}$  led to  $50 \pm 2\%$  inhibition of the NO-stimulated protein (Supporting Information Figure S5) while 1 mM  $\text{Ca}^{2+}$  brought the sGC activity

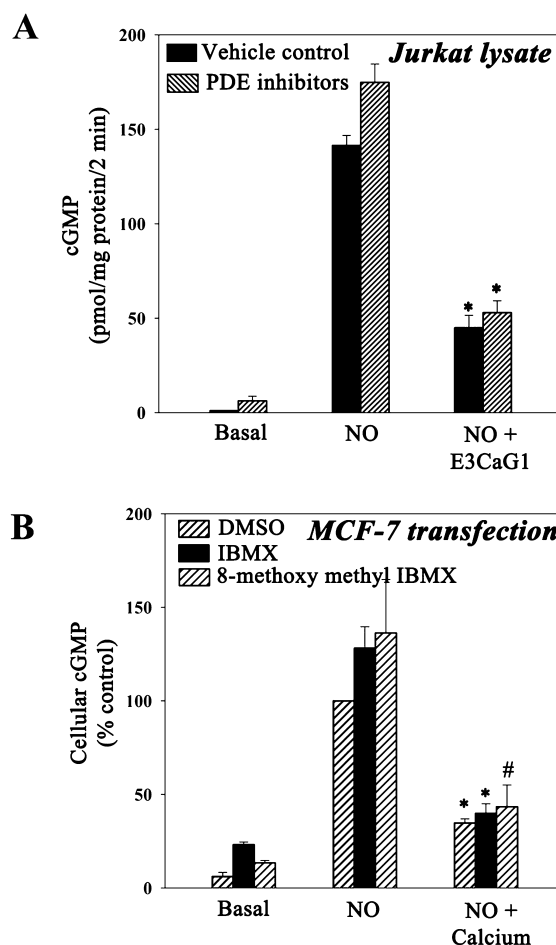


**Figure 6.** Phosphodiesterases are minimally involved in  $\text{Ca}^{2+}$ -dependent lowering of cGMP. (A) Jurkat T cells ( $25 \times 10^6$ ) were incubated with 22 nM E3CaG1 or vehicle control (buffer) for 15 min prior to lysis. Lysates were incubated with IBMX (0.5 mM) and 8-methoxymethyl IBMX (0.4 mM) or vehicle control (DMSO) for 10 min. Following this, Mg-GTP reaction buffer and DEA/NO (10  $\mu\text{M}$ ) were added, and the reaction was stopped after 2 min. Error bars represent the standard deviation from the mean of independent experiments ( $n = 3$ ), and \* denotes  $p < 0.001$ . (B) Transiently transfected MCF-7 cells were incubated with IBMX (0.5 mM), 8-methoxymethyl IBMX (0.4 mM), or DMSO (vehicle control) for 30 min followed by addition of ionomycin (1  $\mu\text{g}/\text{mL}$ ), thapsigargin (400 nM), and calcium chloride (0.1 mM) to appropriate samples, followed immediately by the addition of DEA/NO (10  $\mu\text{M}$ ). After 2 min, cells were spun down and cell pellets frozen. cGMP was measured and expressed in terms of percentage control (10  $\mu\text{M}$  DEA/NO). Error bars represent the standard deviation from the mean of independent experiments ( $n = 3$ ); \* denotes  $p < 0.001$ , and # denotes  $p < 0.01$ .

completely back to basal levels; nanomolar levels of  $\text{Ca}^{2+}$ , as found in vivo, displayed little inhibition in our hands (data not shown). Neither YC-1 nor BAY 41-2272 was able to overcome direct inhibition by 100  $\mu\text{M}$   $\text{Ca}^{2+}$  (Supporting Information Figure S5), in contrast to the inhibition of sGC by E3CaG1 in whole cells. The fact that a high concentration of  $\text{Ca}^{2+}$  is needed to achieve substantial direct inhibition in vitro (micromolar vs nanomolar in the cell) and that YC-1 or BAY 41-2272 does not overcome this inhibition indicates that direct binding of  $\text{Ca}^{2+}$  to sGC does not contribute to the observed intracellular sGC inhibition.



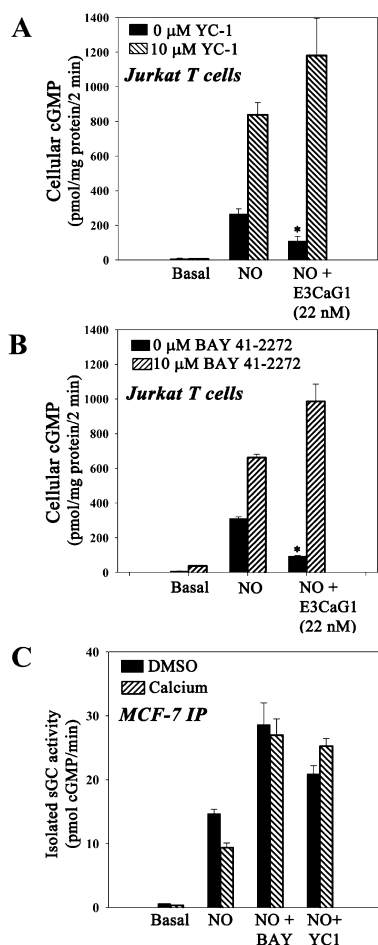


**Figure 7.** Compounds YC-1 and BAY 41-2272 overcome  $\text{Ca}^{2+}$ -dependent inhibition of sGC. (A, B) Jurkat T cells ( $0.5 \times 10^6$ ) were incubated with 22 nM E3CaG1 or buffer for 15 min prior to the addition of 10  $\mu$ M YC-1, 10  $\mu$ M BAY 41-2272, or vehicle control (DMSO). This was followed immediately by the addition of 10  $\mu$ M DEA/NO. Reactions were stopped after 2 min. Both compounds YC-1 and BAY 41-2272 were able to overcome E3CaG1 inhibition of sGC. (C) Transiently transfected MCF-7 cells treated with DMSO or 0.1 mM  $\text{CaCl}_2$  in the presence of ionomycin/thapsigargin. Immunoprecipitated sGC was treated with 10  $\mu$ M YC-1 or 10  $\mu$ M BAY 41-2272, followed immediately by the addition of 10  $\mu$ M DEA/NO. Reactions were carried out at 37  $^\circ\text{C}$  for 5 min, and cGMP accumulation was measured. Error bars represent the standard deviation from the mean of independent experiments ( $n = 5$ ), and \* denotes  $p < 0.001$ .

**Inhibited sGC Exhibits an Increase in  $K_m$ .** To further characterize the inhibited sGC, we measured steady-state kinetic parameters for the protein after immunoprecipitation (Figure 8A and Table 1). The uninhibited protein displayed typical values for  $K_m$  and  $V_{\max}$ <sup>42,46,66,67</sup> and the expected decrease in  $K_m$  and increase in  $V_{\max}$  upon stimulation by NO. In contrast,  $K_m$  values for sGC isolated from calcium-treated cells were dramatically increased and unaltered by NO stimulation (Table 1). The inhibited value ( $K_m \sim 870 \mu\text{M}$ ) is about twice the value for cellular GTP concentrations, which are estimated to be  $\sim 470 \mu\text{M}$  in mammalian tissues.<sup>68</sup> At this GTP concentration, the inhibited protein would operate in the cell at well below  $V_{\max}$ , while the uninhibited protein, with  $K_m = 67 \mu\text{M}$  when bound to NO, would be nearly saturated with GTP and operating at near maximal velocity.

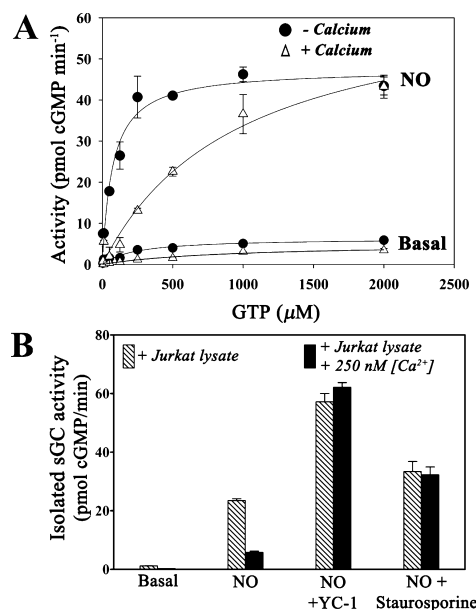


**Figure 8.** Representative kinetic plots for immunoprecipitated sGC obtained from MCF-7 cells. Cells were lysed after treatment for 5 min with ionomycin, thapsigargin, and 2 mM  $\text{CaCl}_2$ , or vehicle control. Reactions were carried out at 37  $^\circ\text{C}$  for 10 min ( $-\text{NO}$ ) or 3 min ( $+\text{NO}$ ). Where included, DEA/NO (50  $\mu$ M) was added just prior to measurement. Shown are the averages of duplicate measurements  $\pm$  the range in measured values. The solid curves represent the nonlinear fit to the Michaelis–Menten equation. (B) Immunoprecipitated sGC treated with Jurkat cell lysate and 250 nM  $\text{Ca}^{2+}$  is inhibited; inhibition is reversed by broad-range protein kinase inhibitor staurosporine. sGC was immunoprecipitated from transiently transfected MCF-7 cells and incubated with Jurkat T cell lysate with or without 250 nM  $\text{Ca}^{2+}$  and/or 1  $\mu$ M staurosporine. Calcium and staurosporine were washed away and cGMP activity was measured. Where indicated, DEA/NO and YC-1 were added to a final concentration of 10  $\mu$ M. Error bars represent the standard deviation from the mean of independent experiments ( $n = 3$ ).

**Table 1. Cellular Calcium-Induced Changes in Kinetic Parameters of sGC<sup>a</sup>**

	$K_{m\text{GTP}}$ ( $\mu\text{M}$ )		$V_{\max}$ (pmol cGMP min <sup>-1</sup> ) <sup>b</sup>		fold increase ( $+\text{Ca}^{2+}/-\text{Ca}^{2+}$ ) <sup>c</sup>	
	$-\text{Ca}^{2+}$	$+\text{Ca}^{2+}$	$-\text{Ca}^{2+}$	$+\text{Ca}^{2+}$	$K_m$	$V_{\max}$
sGC	234 $\pm$ 16	857 $\pm$ 31 <sup>d</sup>	6.3 $\pm$ 1.4	5.1 $\pm$ 0.3 <sup>d</sup>	3.7	0.8
+NO	69 $\pm$ 6	887 $\pm$ 71	41 $\pm$ 9	51 $\pm$ 16	12.9	1.2

<sup>a</sup>Values obtained for immunoprecipitated sGC from MCF-7 cells. Ionomycin, thapsigargin, and 2 mM  $\text{CaCl}_2$ , or vehicle control, was added to the cells 5 min prior to lysis. <sup>b</sup>Presented as pmol min<sup>-1</sup> since the quantity of sGC protein attached to the anti-FLAG agarose beads is unknown. Total lysate protein was  $\sim 65 \mu\text{g}$  per sample. <sup>c</sup>Presented as the ratio of  $+\text{Ca}^{2+}/-\text{Ca}^{2+}$  values. <sup>d</sup>This value is the average  $\pm$  range of two independent experiments performed in duplicate. All other values are the average  $\pm$  standard deviation of three independent experiments performed in duplicate.

**Inhibition of sGC Requires a Calcium-Dependent Kinase.** We developed a cell-free assay for evaluating calcium-dependent inhibition of sGC. Jurkat T cell lysate led to inhibited sGC upon addition of 250 nM  $\text{Ca}^{2+}$  but had no effect in its absence (Figure 8B). Boiling of lysate prior to addition (data not shown), or addition of pan-kinase inhibitor

staurosporine (Figure 8B), prevented inhibition, indicating a calcium-dependent protein kinase was required for inhibition. Obvious candidates for this role are the multifunctional  $\text{Ca}^{2+}$ /calmodulin-dependent protein kinases I, II, and IV. However, addition of compounds KN-62 or KN-93, which inhibit these proteins, had no effect on E3CaG1 inhibition of sGC (data not shown).

## DISCUSSION

The balance between vasoconstriction and vasodilation in mammals, as well as wound healing, angiogenesis, and other related activities, relies on the give-and-take of numerous signaling pathways. Here, we reveal a new level of cross-regulation: TSP-1 and Ang II, two factors of central importance for cell proliferation and vasoconstriction, can inhibit sGC activity by increasing  $[\text{Ca}^{2+}]_i$ . The present experiments were performed in Jurkat T cells, a convenient cell line for these studies since the cells perform well in tissue culture, retain endogenous sGC and also respond to TSP-1 and Ang II. This combination is rare in immortalized cells, which in general do not express sGC. Binding of the TSP-1-derived fragment E3CaG1 to CD47 in Jurkat T cells causes free  $[\text{Ca}^{2+}]_i$  to increase from resting levels of 5–10 nM to peak levels of 300 nM, leading to strong inhibition of sGC (Figures 1–3). Blocking this increase with chelator BAPTA reverses the sGC inhibition (Figure 4B). Inducing an increase in  $[\text{Ca}^{2+}]_i$  with Ang II or PHA (Figure 5), or with the calcium ionophore ionomycin and SERCA inhibitor thapsigargin (Figure 4A), also leads to sGC inhibition. These data make clear that  $\text{Ca}^{2+}$  regulates sGC activity in Jurkat T cells.

The link between Ang II and sGC is particularly interesting to discover. Ang II is part of the renin–angiotensin–aldosterone system for controlling blood pressure through the sensing of blood volume and the linking of kidney function to blood flow.<sup>69</sup> The Ang II receptors are G-protein coupled receptors, the most common of which is angiotensin receptor type 1 ( $\text{AT}_1$ ). Binding leads to an increase in  $[\text{Ca}^{2+}]_i$  through production of inositol triphosphate ( $\text{IP}_3$ ) and subsequent binding to the  $\text{IP}_3$ -sensitive calcium channel of the sarcoplasmic/endoplasmic reticulum. In vascular smooth muscle,  $\text{Ca}^{2+}$  stimulates myosin light chain kinase, which phosphorylates myosin, leading to vasoconstriction. Angiotensin converting enzyme (ACE) inhibitors, and  $\text{AT}_1$  inhibitors, are commonly used to block this pathway and vasoconstriction in the treatment of hypertension.<sup>70</sup> NO-stimulated sGC produces cGMP, which lowers  $[\text{Ca}^{2+}]_i$  through multiple mechanisms, but in particular via phosphorylation of regulatory protein phospholamban by cGMP-dependent protein kinase G (PKG), which leads to stimulation of SERCA and the pumping of  $\text{Ca}^{2+}$  from the cytosol into cellular stores.<sup>71</sup> Interestingly, TSP-1 can also inhibit PKG, further attenuating NO signaling.<sup>72</sup> Additionally, fluctuations in  $[\text{Ca}^{2+}]_i$  may affect the availability of nitric oxide: NADPH oxidase 5 (NOX5), which is found in both vascular smooth muscle and endothelial cells, is stimulated by  $\text{Ca}^{2+}$  to produce superoxide, a free radical molecule that reacts at the diffusion limit with NO to yield peroxynitrite.<sup>73,74</sup> Thus, our data suggest a feedback mechanism that serves to balance vasodilation through NO and vasoconstriction through Ang II by directly raising and lowering  $[\text{Ca}^{2+}]_i$  levels (Figure 9). That this may be the case in vivo is supported by a recent study on Ang II-induced hypertension in

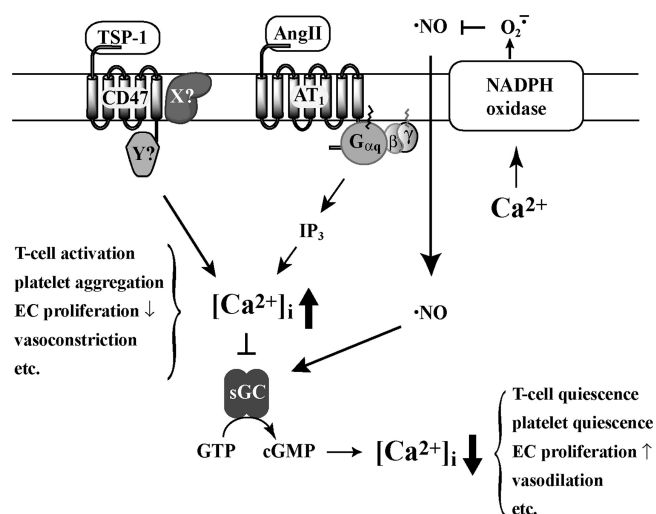


**Figure 9.** Proposed model for influence of  $\text{Ca}^{2+}$  on NO signaling through sGC. Binding of TSP-1 to CD47, or Ang II to  $\text{AT}_1$ , leads to an increase in  $[\text{Ca}^{2+}]_i$ , which inhibits sGC and stimulates NOX5. The proteins associated with CD47 in the signaling complex are not yet identified, shown here as proteins X and Y. NO-stimulation of sGC leads to a decrease in  $[\text{Ca}^{2+}]_i$ . Changes in  $[\text{Ca}^{2+}]_i$  may affect T-cell activation, platelet aggregation, endothelial cell (EC) proliferation, vasodilation, and other cell and tissue specific physiological responses.

rats, which demonstrated that Ang II treatment led to blunted sGC activity.<sup>75</sup>

A major finding in the present study is that increased  $[\text{Ca}^{2+}]_i$  leads to inhibition of sGC through covalent modification, most likely by phosphorylation. sGC inhibited in Jurkat T or MCF-7 cells (Figures 6 and 7), or in Jurkat lysate supplemented with 250 nM  $\text{Ca}^{2+}$  (Figure 8), remains inhibited after the excess calcium is diluted or washed away, displaying a 13-fold increase in  $K_{\text{mGTP}}$  in the presence of NO (Figure 8 and Table 1). Inhibition of kinases with staurosporine relieves the calcium-dependent inhibition of sGC (Figure 8), suggesting inhibition is through direct phosphorylation of sGC. Interestingly, TSP-1-dependent inhibition of PKG also appears to be through covalent modification since inhibition is retained in cell-free extracts,<sup>72</sup> indicating a common mechanism may be at work. Although  $\text{Ca}^{2+}$  can also stimulate  $\text{Ca}^{2+}$ /calmodulin-dependent phosphodiesterases, particularly in neuronal cell extracts,<sup>43</sup> phosphodiesterase activity is at most a minor contributor to the inhibition observed in the present experiments.

sGC allosteric activators YC-1 and BAY 41-2272, which are synergistic with CO and NO for stimulating sGC activity, completely restore NO-stimulated sGC activity. The compounds overcome E3CaG1 inhibition of sGC in Jurkat T cells (Figure 7A,B) and overcome calcium-induced inhibition of sGC in MCF-7 cells (Figure 7C) or in cell lysate (Figure 8B). These results suggest the sGC modification leads to a protein that is stabilized in a low activity conformation but still fully capable of catalysis. Allosteric stimulation by NO alone is insufficient to drive the modified protein into a fully active state, but in combination with YC-1 or BAY 41-2272, full activity is achieved. Similarly, recent data from Miller and co-workers indicate that stimulation of sGC by YC-1 and BAY 41-2272 in TSP-1-treated platelets and vascular smooth muscle cells is reduced, as was stimulation by NO alone;<sup>76</sup> however, stimulation with both YC-1 and NO was not examined in that

study. Taken together, these data indicate that both allosteric activator and NO are required to completely overcome TSP-1-dependent inhibition. The data also suggest that the YC-1 class of compounds may offer broad relief to hypertensive individuals, even where Ang II and TSP-1 levels are high, as occurs, for example, in older individuals or those suffering from type II diabetes.<sup>70,77</sup>

The mechanism by which TSP-1/E3CaG1 causes increases in  $[Ca^{2+}]_i$  remains unknown. CD47 is clearly required for signal transduction (Figure 3). However, E3CaG1 binding is lost as Jurkat T cells age despite the continued presence of CD47 on the cell surface (Figure 1), suggesting that CD47 alone may not be sufficient for binding and signaling. CD47 was originally identified as integrin associated protein and is likely to function through a signaling complex. Interestingly, CD47 is required for integrin-mediated  $Ca^{2+}$  influx in endothelial cells,<sup>78</sup> which may be related to the  $Ca^{2+}$  signal described herein. Several integrin complexes are known to induce  $Ca^{2+}$  influx,<sup>79–81</sup> although others reduce  $[Ca^{2+}]_i$ .<sup>81</sup> CD47 may also associate with  $G_i$  protein and thereby function as a noncanonical GPCR.<sup>15</sup> In such a mechanism, binding of TSP-1/E3CaG1 would induce  $Ca^{2+}$  mobilization through  $IP_3$ , much as happens with Ang II binding to  $AT_1$ . However, pertussis toxin had no effect on  $Ca^{2+}$  mobilization (Figure S4) or inhibition of sGC in Jurkat T cells, suggesting  $G_i$  is not involved, and initial experiments designed to interfere with specific integrins did not alter E3CaG1-dependent  $Ca^{2+}$  mobilization (Figure 3C and Figure S4). Furthermore, TSP-1 transiently decreases  $IP_3$  in A2058 melanoma cells.<sup>82</sup>

Finally, it should be noted that autocrine NO signaling, which occurs in endothelial and neuronal cells, is complicated with respect to  $Ca^{2+}$ . Increased  $[Ca^{2+}]_i$  stimulates eNOS and nNOS, leading to NO production, yet also inhibits sGC. Recent experiments by Isenberg and co-workers using endothelial cells demonstrated that TSP-1 binding through CD47 led to a decrease in the ability of ionomycin to increase  $[Ca^{2+}]_i$  and a subsequent decrease in NO production by eNOS.<sup>83</sup>

In summary, we have shown that sGC is inhibited by a cellular increase in calcium, which can be induced by extracellular TSP-1 fragment E3CaG1 binding to transmembrane protein CD47 and associated proteins, or by Ang II binding to  $AT_1$ . This inhibition of NO-stimulated sGC involves a post-translational modification and can be overcome through the binding of allosteric compounds YC-1 and BAY 41-2272.

## ■ ASSOCIATED CONTENT

### ● Supporting Information

Figures S1–S5 and movie M1. This material is available free of charge via the Internet at <http://pubs.acs.org>.

## ■ AUTHOR INFORMATION

### Corresponding Author

\*Tel: (520) 621-1884. Fax: (520) 626-9204. E-mail: [montfort@email.arizona.edu](mailto:montfort@email.arizona.edu).

### Funding

This work was supported by grants from the American Heart Association (09POST2150120 to S.M.), from the National Institutes of Health (T32 HL07249 to S.M., R01 HL062969 and U54 CA143924 to W.R.M., ES 04940 to S.B.), and from the Semiconductor Research Corporation (projects 425.023; 425.024 to S.B.). Flow cytometry was performed in

the AZCC/ARL-Division of Biotechnology Cytometry Core Facility (supported by NIH grant CA023074).

## ■ ACKNOWLEDGMENTS

We are grateful to Deanne Mosher and Doug Annis for generously providing their E3CaG1 expression virus and purification protocols, to Xiaohui Hu for preparing the initial human sGC expression constructs, to David Roberts and Thomas Miller for JinB8 and Jurkat A1 cell lines, and to Jacquie Brailey and Andrzej Weichsel for excellent technical support.

## ■ ABBREVIATIONS

sGC, soluble guanylyl cyclase; DEA/NO, 2-(*N,N*-diethylamino)-diazene-2-oxide; TSP-1, thrombospondin-1; FITC, fluorescein isothiocyanate; FACS, fluorescence activated cell sorting;  $[Ca^{2+}]_i$ , cytosolic calcium concentration; SERCA, sarco/endoplasmic reticulum  $Ca^{2+}$  ATPase; Ang II, Angiotensin II; PHA, phytohemagglutinin; BAPTA-AM, acetoxymethyl ester derivative of 1,2-bis(*o*-aminophenoxy)ethane-*N,N,N',N'*-tetraacetic acid); PKG, cGMP-dependent protein kinase G; GPCR, G-protein coupled receptor; IBMX, 3-isobutyl-1-methylxanthine.

## ■ REFERENCES

- (1) Ignarro, L. J. (2000) *Nitric Oxide Biology and Pathobiology*, Academic Press, San Diego, CA.
- (2) Li, H., and Poulos, T. L. (2005) Structure-function studies on nitric oxide synthases. *J. Inorg. Biochem.* 99, 293–305.
- (3) Stuehr, D. J., Tejero, J., and Haque, M. M. (2009) Structural and mechanistic aspects of flavoproteins: electron transfer through the nitric oxide synthase flavoprotein domain. *FEBS J.* 276, 3959–3974.
- (4) Pyriochou, A., and Papapetropoulos, A. (2005) Soluble guanylyl cyclase: more secrets revealed. *Cell. Signalling* 17, 407–413.
- (5) Russwurm, M., and Koesling, D. (2004) Guanylyl cyclase: NO hits its target. *Biochem. Soc. Symp.* 71, 51–63.
- (6) Boon, E. M., and Marletta, M. A. (2005) Ligand specificity of H-NOX domains: from sGC to bacterial NO sensors. *J. Inorg. Biochem.* 99, 892–902.
- (7) Martin, E., Berka, V., Tsai, A. L., and Murad, F. (2005) Soluble guanylyl cyclase: the nitric oxide receptor. *Methods Enzymol.* 396, 478–492.
- (8) Schulz, R., Rassaf, T., Massion, P. B., Kelm, M., and Balligand, J. L. (2005) Recent advances in the understanding of the role of nitric oxide in cardiovascular homeostasis. *Pharmacol. Ther.* 108, 225–256.
- (9) Isenberg, J. S., Ridnour, L. A., Dimitry, J., Frazier, W. A., Wink, D. A., and Roberts, D. D. (2006) CD47 is necessary for inhibition of nitric oxide-stimulated vascular cell responses by thrombospondin-1. *J. Biol. Chem.* 281, 26069–26080.
- (10) Isenberg, J. S., Roberts, D. D., and Frazier, W. A. (2008) CD47: a new target in cardiovascular therapy. *Arterioscler. Thromb. Vasc. Biol.* 28, 615–621.
- (11) Kaur, S., Martin-Manso, G., Pendrak, M. L., Garfield, S. H., Isenberg, J. S., and Roberts, D. D. (2010) Thrombospondin-1 Inhibits VEGF Receptor-2 Signaling by Disrupting Its Association with CD47. *J. Biol. Chem.* 285, 38923–38932.
- (12) Bornstein, P. (2009) Thrombospondins function as regulators of angiogenesis. *J. Cell Commun. Signal* 3, 189–200.
- (13) Bonnefoy, A., Moura, R., and Hoylaerts, M. F. (2008) The evolving role of thrombospondin-1 in hemostasis and vascular biology. *Cell. Mol. Life Sci.* 65, 713–727.
- (14) Carlson, C. B., Lawler, J., and Mosher, D. F. (2008) Structures of thrombospondins. *Cell. Mol. Life Sci.* 65, 672–686.



- (15) Brown, E. J., and Frazier, W. A. (2001) Integrin-associated protein (CD47) and its ligands. *Trends Cell Biol.* 11, 130–135.
- (16) Oldenborg, P. A., Zheleznyak, A., Fang, Y. F., Lagenaur, C. F., Gresham, H. D., and Lindberg, F. P. (2000) Role of CD47 as a marker of self on red blood cells. *Science* 288, 2051–2054.
- (17) Frazier, W. A., Gao, A. G., Dimitry, J., Chung, J., Brown, E. J., Lindberg, F. P., and Linder, M. E. (1999) The thrombospondin receptor integrin-associated protein (CD47) functionally couples to heterotrimeric Gi. *J. Biol. Chem.* 274, 8554–8560.
- (18) Manna, P. P., and Frazier, W. A. (2004) CD47 mediates killing of breast tumor cells via Gi-dependent inhibition of protein kinase A. *Cancer Res.* 64, 1026–1036.
- (19) Manna, P. P., and Frazier, W. A. (2003) The mechanism of CD47-dependent killing of T cells: heterotrimeric Gi-dependent inhibition of protein kinase A. *J. Immunol.* 170, 3544–3553.
- (20) Landry, Y., Niederhoffer, N., Sick, E., and Gies, J. P. (2006) Heptahelical and other G-protein-coupled receptors (GPCRs) signaling. *Curr. Med. Chem.* 13, 51–63.
- (21) Isenberg, J. S., Ridnour, L. A., Perruccio, E. M., Espey, M. G., Wink, D. A., and Roberts, D. D. (2005) Thrombospondin-1 inhibits endothelial cell responses to nitric oxide in a cGMP-dependent manner. *Proc. Natl. Acad. Sci. U.S.A.* 102, 13141–13146.
- (22) Isenberg, J. S., Wink, D. A., and Roberts, D. D. (2006) Thrombospondin-1 antagonizes nitric oxide-stimulated vascular smooth muscle cell responses. *Cardiovasc. Res.* 71, 785–793.
- (23) Sick, E., Niederhoffer, N., Takeda, K., Landry, Y., and Gies, J. P. (2009) Activation of CD47 receptors causes histamine secretion from mast cells. *Cell. Mol. Life Sci.* 66, 1271–1282.
- (24) Tsao, P. W., and Mousa, S. A. (1995) Thrombospondin mediates calcium mobilization in fibroblasts via its Arg-Gly-Asp and carboxyl-terminal domains. *J. Biol. Chem.* 270, 23747–23753.
- (25) Poulos, T. L. (2006) Soluble guanylate cyclase. *Curr. Opin. Struct. Biol.* 16, 736–743.
- (26) Wykes, V., and Garthwaite, J. (2004) Membrane-association and the sensitivity of guanylyl cyclase-coupled receptors to nitric oxide. *Br. J. Pharmacol.* 141, 1087–1090.
- (27) Agulló, L., Garcia-Dorado, D., Escalona, N., Ruiz-Meana, M., Mirabet, M., Inserte, J., and Soler-Soler, J. (2005) Membrane association of nitric oxide-sensitive guanylyl cyclase in cardiomyocytes. *Cardiovasc. Res.* 68, 65–74.
- (28) Zabel, U., Hausler, C., Weeger, M., and Schmidt, H. H. (1999) Homodimerization of soluble guanylyl cyclase subunits. Dimerization analysis using a glutathione s-transferase affinity tag. *J. Biol. Chem.* 274, 18149–18152.
- (29) Zwiller, J., Revel, M. O., and Basset, P. (1981) Evidence for phosphorylation of rat brain guanylate cyclase by cyclic AMP-dependent protein kinase. *Biochem. Biophys. Res. Commun.* 101, 1381–1387.
- (30) Zhou, Z., Sayed, N., Pyriochou, A., Roussos, C., Fulton, D., Beuve, A., and Papapetropoulos, A. (2008) Protein kinase G phosphorylates soluble guanylyl cyclase on serine 64 and inhibits its activity. *Arterioscler. Thromb. Vasc. Biol.* 28, 1803–1810.
- (31) Murthy, K. S. (2001) Activation of phosphodiesterase 5 and inhibition of guanylate cyclase by cGMP-dependent protein kinase in smooth muscle. *Biochem. J.* 360, 199–208.
- (32) Murthy, K. S. (2008) Inhibitory phosphorylation of soluble guanylyl cyclase by muscarinic m2 receptors via Gbetagamma-dependent activation of c-Src kinase. *J. Pharmacol. Exp. Ther.* 325, 183–189.
- (33) Ferrero, R., Rodriguez-Pascual, F., Miras-Portugal, M. T., and Torres, M. (2000) Nitric oxide-sensitive guanylyl cyclase activity inhibition through cyclic GMP-dependent dephosphorylation. *J. Neurochem.* 75, 2029–2039.
- (34) Kostic, T. S., Andric, S. A., and Stojilkovic, S. S. (2004) Receptor-controlled phosphorylation of alpha 1 soluble guanylyl cyclase enhances nitric oxide-dependent cyclic guanosine 5'-monophosphate production in pituitary cells. *Mol. Endocrinol.* 18, 458–470.
- (35) Russwurm, M., Wittau, N., and Koesling, D. (2001) Guanylyl cyclase/PSD-95 interaction: targeting of the nitric oxide-sensitive alpha2beta1 guanylyl cyclase to synaptic membranes. *J. Biol. Chem.* 276, 44647–44652.
- (36) Papapetropoulos, A., Zhou, Z., Gerassimou, C., Yetik, G., Venema, R. C., Roussos, C., Sessa, W. C., and Catravas, J. D. (2005) Interaction between the 90-kDa heat shock protein and soluble guanylyl cyclase: physiological significance and mapping of the domains mediating binding. *Mol. Pharmacol.* 68, 1133–1141.
- (37) Meurer, S., Pioch, S., Gross, S., and Muller-Esterl, W. (2005) Reactive oxygen species induce tyrosine phosphorylation of and Src kinase recruitment to NO-sensitive guanylyl cyclase. *J. Biol. Chem.* 280, 33149–33156.
- (38) Gambaryan, S., Kobsar, A., Hartmann, S., Birschmann, I., Kuhlencordt, P. J., Muller-Esterl, W., Lohmann, S. M., and Walter, U. (2008) NO-synthase-/NO-independent regulation of human and murine platelet soluble guanylyl cyclase activity. *J. Thromb. Haemost.* 6, 1376–1384.
- (39) Sayed, N., Baskaran, P., Ma, X., van den Akker, F., and Beuve, A. (2007) Desensitization of soluble guanylyl cyclase, the NO receptor, by S-nitrosylation. *Proc. Natl. Acad. Sci. U.S.A.* 104, 12312–12317.
- (40) Mayer, B., Kleschyov, A. L., Stessel, H., Russwurm, M., Munzel, T., Koesling, D., and Schmidt, K. (2009) Inactivation of soluble guanylate cyclase by stoichiometric S-nitrosation. *Mol. Pharmacol.* 75, 886–891.
- (41) Parkinson, S. J., Jovanovic, A., Jovanovic, S., Wagner, F., Terzic, A., and Waldman, S. A. (1999) Regulation of nitric oxide-responsive recombinant soluble guanylyl cyclase by calcium. *Biochemistry* 38, 6441–6448.
- (42) Serfass, L., Carr, H. S., Aschenbrenner, L. M., and Burstyn, J. N. (2001) Calcium ion downregulates soluble guanylyl cyclase activity: evidence for a two-metal ion catalytic mechanism. *Arch. Biochem. Biophys.* 387, 47–56.
- (43) Mayer, B., Klatt, P., Bohme, E., and Schmidt, K. (1992) Regulation of neuronal nitric oxide and cyclic GMP formation by Ca<sup>2+</sup>. *J. Neurochem.* 59, 2024–2029.
- (44) James, L. R., Griffiths, C. H., Garthwaite, J., and Bellamy, T. C. (2009) Inhibition of nitric oxide-activated guanylyl cyclase by calmodulin antagonists. *Br. J. Pharmacol.* 158, 1454–1464.
- (45) Andric, S. A., Kostic, T. S., Tomic, M., Koshimizu, T., and Stojilkovic, S. S. (2001) Dependence of soluble guanylyl cyclase activity on calcium signaling in pituitary cells. *J. Biol. Chem.* 276, 844–849.
- (46) Kazeronian, S., Pitari, G. M., Ruiz-Stewart, I., Schulz, S., and Waldman, S. A. (2002) Nitric oxide activation of soluble guanylyl cyclase reveals high and low affinity sites that mediate allosteric inhibition by calcium. *Biochemistry* 41, 3396–3404.
- (47) Iversen, B. M., and Arendshorst, W. J. (1998) ANG II and vasopressin stimulate calcium entry in dispersed smooth muscle cells of preglomerular arterioles. *Am. J. Physiol.* 274, F498–F508.
- (48) Kang, M., Chung, K. Y., and Walker, J. W. (2007) G-protein coupled receptor signaling in myocardium: not for the faint of heart. *Physiology* 22, 174–184.
- (49) Ticchioni, M., Raimondi, V., Lamy, L., Wijdenes, J., Lindberg, F. P., Brown, E. J., and Bernard, A. (2001) Integrin-associated protein (CD47/IAP) contributes to T cell arrest on inflammatory vascular endothelium under flow. *FASEB J.* 15, 341–350.
- (50) Romzek, N. C., Harris, E. S., Dell, C. L., Skronek, J., Hasse, E., Reynolds, P. J., Hunt, S. W. 3rd, and Shimizu, Y. (1998) Use of a beta1 integrin-deficient human T cell to identify beta1 integrin cytoplasmic domain sequences critical for integrin function. *Mol. Biol. Cell* 9, 2715–2727.

- (51) Mosher, D. F., Huwiler, K. G., Misenheimer, T. M., and Annis, D. S. (2002) Expression of recombinant matrix components using baculoviruses. *Methods Cell. Biol.* 69, 69–81.
- (52) Pruitt, K. D., Harrow, J., Harte, R. A., Wallin, C., Diekhans, M., Maglott, D. R., Searle, S., Farrell, C. M., Loveland, J. E., Ruef, B. J., Hart, E., Suner, M. M., Landrum, M. J., Aken, B., Ayling, S., Baertsch, R., Fernandez-Banet, J., Cherry, J. L., Curwen, V., Dicuccio, M., Kellis, M., Lee, J., Lin, M. F., Schuster, M., Shkeda, A., Amid, C., Brown, G., Dukhanina, O., Frankish, A., Hart, J., Maidak, B. L., Mudge, J., Murphy, M. R., Murphy, T., Rajan, J., Rajput, B., Riddick, L. D., Snow, C., Steward, C., Webb, D., Weber, J. A., Wilming, L., Wu, W., Birney, E., Haussler, D., Hubbard, T., Ostell, J., Durbin, R., and Lipman, D. (2009) The consensus coding sequence (CCDS) project: Identifying a common protein-coding gene set for the human and mouse genomes. *Genome Res.* 19, 1316–1323.
- (53) Grynkiewicz, G., Poenie, M., and Tsien, R. Y. (1985) A new generation of Ca<sup>2+</sup> indicators with greatly improved fluorescence properties. *J. Biol. Chem.* 260, 3440–3450.
- (54) Isenberg, J. S., Annis, D. S., Pendrak, M. L., Ptaszynska, M., Frazier, W. A., Mosher, D. F., and Roberts, D. D. (2009) Differential interactions of thrombospondin-1, -2, and -4 with CD47 and effects on cGMP signaling and ischemic injury responses. *J. Biol. Chem.* 284, 1116–1125.
- (55) Schottelndreier, H., Potter, B. V., Mayr, G. W., and Guse, A. H. (2001) Mechanisms involved in alpha6beta1-integrin-mediated Ca(2+) signalling. *Cell. Signal* 13, 895–899.
- (56) Fischer, B. S., Qin, D., Kim, K., and McDonald, T. V. (2001) Capsaicin inhibits Jurkat T-cell activation by blocking calcium entry current I(CRAC). *J. Pharmacol. Exp. Ther.* 299, 238–246.
- (57) Apostolakis, S., Vlata, Z., Vogiatzi, K., Krambovitis, E., and Spandidos, D. A. (2010) Angiotensin II up-regulates CX3CR1 expression in THP-1 monocytes: impact on vascular inflammation and atherogenesis. *J. Thromb. Thrombolysis* 29, 443–448.
- (58) Haubert, D., and Weckbecker, G. (2010) Vav1 couples the T cell receptor to cAMP response element activation via a PKC-dependent pathway. *Cell. Signalling* 22, 944–954.
- (59) Evgenov, O. V., Pacher, P., Schmidt, P. M., Hasko, G., Schmidt, H. H., and Stasch, J. P. (2006) NO-independent stimulators and activators of soluble guanylate cyclase: discovery and therapeutic potential. *Nat. Rev. Drug Discovery* 5, 755–768.
- (60) Mittendorf, J., Weigand, S., Alonso-Alija, C., Bischoff, E., Feurer, A., Gerisch, M., Kern, A., Knorr, A., Lang, D., Muentner, K., Radtke, M., Schirok, H., Schlemmer, K. H., Stahl, E., Straub, A., Wunder, F., and Stasch, J. P. (2009) Discovery of riociguat (BAY 63–2521): a potent, oral stimulator of soluble guanylate cyclase for the treatment of pulmonary hypertension. *ChemMedChem* 4, 853–865.
- (61) Friebe, A., Mullershausen, F., Smolenski, A., Walter, U., Schultz, G., and Koesling, D. (1998) YC-1 potentiates nitric oxide- and carbon monoxide-induced cyclic GMP effects in human platelets. *Mol. Pharmacol.* 54, 962–967.
- (62) Galle, J., Zabel, U., Hubner, U., Hatzelmann, A., Wagner, B., Wanner, C., and Schmidt, H. H. (1999) Effects of the soluble guanylyl cyclase activator, YC-1, on vascular tone, cyclic GMP levels and phosphodiesterase activity. *Br. J. Pharmacol.* 127, 195–203.
- (63) Mullershausen, F., Russwurm, M., Friebe, A., and Koesling, D. (2004) Inhibition of phosphodiesterase type 5 by the activator of nitric oxide-sensitive guanylyl cyclase BAY 41-2272. *Circulation* 109, 1711–1713.
- (64) Bischoff, E., and Stasch, J. P. (2004) Effects of the sGC stimulator BAY 41-2272 are not mediated by phosphodiesterase 5 inhibition. *Circulation* 110, e320–321; authorreply e320–321.
- (65) Stasch, J.-P., Becker, E. M., Alonso-Alija, C., Apeler, H., Gerzer, R., Minuth, T., Perzborn, E., Pleiss, U., Schröder, H., Schroeder, W., Stahl, E., Steinke, W., Straub, A., and Schramm, M. (2001) NO-independent regulatory site on soluble guanylate cyclase. *Nature* 410, 212–215.
- (66) Denninger, J. W., Schelvis, J. P. M., Brandish, P. E., Zhao, Y., Babcock, G. T., and Marletta, M. A. (2000) Interaction of soluble guanylate cyclase with YC-1: Kinetic and resonance Raman studies. *Biochemistry* 39, 4191–4198.
- (67) Chang, F. J., Lemme, S., Sun, Q., Sunahara, R. K., and Beuve, A. (2005) Nitric oxide-dependent allosteric inhibitory role of a second nucleotide binding site in soluble guanylyl cyclase. *J. Biol. Chem.* 280, 11513–11519.
- (68) Traut, T. W. (1994) Physiological concentrations of purines and pyrimidines. *Mol. Cell. Biochem.* 140, 1–22.
- (69) Castrop, H., Hoerl, K., Kurtz, A., Schweda, F., Todorov, V., and Wagner, C. (2010) Physiology of kidney renin. *Physiol. Rev.* 90, 607–673.
- (70) Shi, L., Mao, C., Xu, Z., and Zhang, L. (2010) Angiotensin-converting enzymes and drug discovery in cardiovascular diseases. *Drug Discovery Today* 15, 332–341.
- (71) Traaseth, N. J., Ha, K. N., Verardi, R., Shi, L., Buffy, J. J., Masterson, L. R., and Veglia, G. (2008) Structural and dynamic basis of phospholamban and sarcolipin inhibition of Ca(2+)-ATPase. *Biochemistry* 47, 3–13.
- (72) Isenberg, J. S., Romeo, M. J., Yu, C., Yu, C. K., Nghiem, K., Monsale, J., Rick, M. E., Wink, D. A., Frazier, W. A., and Roberts, D. D. (2008) Thrombospondin-1 stimulates platelet aggregation by blocking the antithrombotic activity of nitric oxide/cGMP signaling. *Blood* 111, 613–623.
- (73) Sumimoto, H. (2008) Structure, regulation and evolution of Nox-family NADPH oxidases that produce reactive oxygen species. *FEBS J.* 275, 3249–3277.
- (74) Bedard, K., and Krause, K. H. (2007) The NOX family of ROS-generating NADPH oxidases: physiology and pathophysiology. *Physiol. Rev.* 87, 245–313.
- (75) Bae, E. H., Ma, S. K., Lee, J., and Kim, S. W. (2011) Altered regulation of renal nitric oxide and atrial natriuretic peptide systems in angiotensin II-induced hypertension. *Regul. Pept.* 170, 31–37.
- (76) Miller, T. W., Isenberg, J. S., and Roberts, D. D. (2010) Thrombospondin-1 is an inhibitor of pharmacological activation of soluble guanylate cyclase. *Br. J. Pharmacol.* 159, 1542–1547.
- (77) Isenberg, J. S., Frazier, W. A., and Roberts, D. D. (2008) Thrombospondin-1: a physiological regulator of nitric oxide signaling. *Cell. Mol. Life Sci.* 65, 728–742.
- (78) Schwartz, M. A., Brown, E. J., and Fazeli, B. (1993) A 50-kDa integrin-associated protein is required for integrin-regulated calcium entry in endothelial cells. *J. Biol. Chem.* 268, 1–19934.
- (79) Mariko, B., Ghandour, Z., Raveaud, S., Quentin, M., Usson, Y., Verdeti, J., Huber, P., Kielty, C., and Faury, G. (2010) Microfibrils and fibrillin-1 induce integrin-mediated signaling, proliferation and migration in human endothelial cells. *Am. J. Physiol. Cell Physiol.* .
- (80) Sjaastad, M. D., and Nelson, W. J. (1997) Integrin-mediated calcium signaling and regulation of cell adhesion by intracellular calcium. *Bioessays* 19, 47–55.
- (81) Davis, M. J., Wu, X., Nurkiewicz, T. R., Kawasaki, J., Gui, P., Hill, M. A., and Wilson, E. (2002) Regulation of ion channels by integrins. *Cell Biochem. Biophys.* 36, 41–66.
- (82) Guo, N., Zabrenetzky, V. S., Chandrasekaran, L., Sipes, J. M., Lawler, J., Krutzsch, H. C., and Roberts, D. D. (1998) Differential roles of protein kinase C and pertussis toxin-sensitive G-binding proteins in modulation of melanoma cell proliferation and motility by thrombospondin 1. *Cancer Res.* 58, 3154–3162.
- (83) Bauer, E. M., Qin, Y., Miller, T. W., Bandle, R. W., Csanyi, G., Pagano, P. J., Bauer, P. M., Schnermann, J., Roberts, D. D., and Isenberg, J. S. (2010) Thrombospondin-1 supports blood pressure by limiting eNOS activation and endothelial-dependent vasorelaxation. *Cardiovasc. Res.* 88, 471–481.